Proceedings of the Seventh International Conference on
Railway Technology: Research, Development and Maintenance
Edited by: J. Pombo
Civil-Comp Conferences, Volume 15, Paper 16.4
Civil-Comp Press, Edinburgh, United Kingdom, 2026
ISSN: 2753-3239, doi: 10.4203/ccc.15.16.4

Speed Control of a Freight Train Based on an Inverse Simulation Approach

A. Mcgirr, E. Mcgookin, D. Thomson and D. Murray-Smith

James Watt School of Engineering, University of Glasgow, United Kingdom

Abstract

This paper discusses the use of Inverse Simulation (IS) techniques based on feedback control to develop a more effective driving strategy for a demanding route for a freight rail vehicle. A multi-dynamic mathematical model of a G-Scale freight locomotive and wagon is developed and implemented in this study. The framework for the IS and the accompanying simulation implementation is shown. Results for a test route comprised of gradients and a sharp curve are presented. Finally, some conclusions are drawn regarding the use of IS in this context.

Keywords: rail vehicle, inverse simulation, driving strategy, feedback principles, mathematical model, curve radius, gradient

1 Introduction

Advances in rail vehicle modelling and autonomous control have attracted interest in developing more effective driving strategies/algorithms that would enhance various aspects of rail vehicle performance. These include journey time, power/fuel consumption or reducing wear of components, such as wheelsets [1]. This involves a demanded tractive force level and adjustment of the associated control inputs of the vehicle, which directly affects the power consumed and the speed of the vehicle. Adjustment of these controls would depend on several factors, such as the current or upcoming route profile, weather conditions, speed restriction and coaches/wagon configuration.

Modelling and simulation of rail vehicles in the context of driving style and scheduling purposes is well established and is aptly named Longitudinal Train Dynamics (LTD) [2]. Several advanced control systems have been developed using these models and have shown to be successful in improving the driving strategy. For example, a hybrid algorithm involving PID and fuzzy control has been found to improve the fuel consumption of a diesel-electric locomotive, with minimal impacts on journey time [1]. The control strategy adopted in this paper is Inverse Simulation (IS). This involves defining the desired trajectory/response of the vehicle and constructing the required control inputs for the manoeuvre [3]. In the context of trains, since the speed restrictions and route characteristics are all pre-determined, this allows an IS framework to be implemented. The IS method allows the tractive force levels to be estimated to traverse a given series of track features. The test route considered in this paper incorporates some of the most demanding features that a rail vehicle can encounter. The IS approach can be applied equally well to real routes such as those found in the West Highlands of Scotland, which are characterized by long uphill sections and sharp curvature [4]. The work described in this paper involves the mathematical modelling, simulation and testing of the longitudinal and lateral dynamic models of a G-scale BR232 freight locomotive and Gondola wagon, which allows motor parameters to be accurately known and therefore produce reliable tractive force trends.

This paper is structured as follows: Section 2 briefly outlines the mathematical model used in the work and the implementation of the IS framework. Section 3 provides some results from the model and compares them to the route being traversed without any control structure in place. The results and their implementation in the real system are also discussed in Section 3. Finally, the conclusions and primary contributions from the work are described in Section 4.

2 Methods

For analysis of the driving strategy of a freight train, a suitable mathematical model is required to allow testing on longer routes that are not achievable practically. Traditional longitudinal models for freight vehicles are based on the use of point mass assumptions, either for the entire train or for each unit, where the inter-vehicle connections are standard mass-spring-damper systems [5]. The model used in this work takes these principles one step further, where the major components within the vehicle are given their own dynamics, and are connected to neighbouring components. The main chosen components of the locomotive considered are the four powered wheelsets, the two three-axle bogie frames and the main body, which houses the motors, lighting elements and electronics systems. The major chosen components of the wagon model are the two bogies and the wagon body, which includes a container that can be empty or loaded appropriately. The track parameters change for each component of the locomotive and wagon sub-models as they are encountered, resulting in a gradual change in the characteristics of the overall train model as new track curvature and grade resistance values are applied. The first iteration of this form of simulation model can therefore be regarded as a natural evolution of point-mass and multi-mass models. The train used as part of the study can be seen in Figure 1.

2.1 Rigid Body Dynamics

The rigid-body dynamics of each component in the vehicle are governed by the Newton-Euler equations described by Fossen [6] and McGookin [7]. These describe the implementation of the forces and torques acting on the body and the corresponding kinematic transformations between the Body-Fixed frame and the Earth-Fixed frame.

$$\dot{\mathbf{x}}=\begin{bmatrix}\dot{\mathbf{v}}\\ \dot{\boldsymbol{\eta}}\end{bmatrix}=\begin{bmatrix}-\mathbf{M}^{-1}[(\mathbf{C}+\mathbf{D})\mathbf{v}+\mathbf{g}(\boldsymbol{\eta})-\boldsymbol{\tau}\\ \mathbf{J}(\boldsymbol{\eta})\mathbf{v}\end{bmatrix} \tag{1}$$

Here, $\mathbf{M}$ is the mass and inertia matrix, $\mathbf{C}$ is the Coriolis matrix, $\mathbf{D}$ is the damping matrix, $\mathbf{v}$ is the velocities vector, $\boldsymbol{\eta}$ is the vector containing the position and angular parameters, $\mathbf{g}(\boldsymbol{\eta})$ is a vector describing the forces and moments acting on the body due to gravity and $\boldsymbol{\tau}$ is a vector describing the forces and moments acting on the body due to actuators or other external forces. $\mathbf{J}(\boldsymbol{\eta})$ is an Euler matrix describing how the Body-Fixed reference frame maps onto the Earth-Fixed reference frame [8].

(a) BR232 Locomotive (b) Gondola Wagon

Figure 1: G-Scale Train Used in the Work

2.2 Longitudinal Train Dynamics

The standard form of LTD treats suspension elements as one component 'leading' and the other 'trailing' e.g. a locomotive pulling a wagon. The same principle is adopted here e.g. a wheelset pulling a bogie frame, or a bogie frame pulling the carbody. The general form of the forces acting on the components is given below in Equations (2) and (3).

$$F_{s,l} = k_s(s_L-(s_T+s_0))+c_s(\dot{s}_L-\dot{s}_T) \tag{2}$$

$$F_{s,t} = k_s((s_T+s_0)-s_L)+c_s(\dot{s}_T-\dot{s}_L) \tag{3}$$

Here, $F_{s,l}$ is the force acting on the leading component (N) and $F_{s,t}$ is the force acting on the trailing component (N), k_s is the spring stiffness (1000 N/m between locomotive wheelset and bogie frame, 2500 N/m between bogie frame and carbody and 500 N/m between wagon bogie frame and container), s_L and s_T are the inertial positions of the leading and trailing component (m), s_0 is the difference between the inertial positions of both components (the addition to the trailing component position ensures that relative displacements remain small) (m), c_s is the damping coefficient (100 Ns/m between locomotive wheelset and bogie frame, 250 Ns/m between bogie frame and carbody and 10 Ns/m between wagon bogie frame and container), $\dot{s}_l$ and $\dot{s}_t$ are the velocities of the leading and trailing component (m/s), respectively (taken to be the resultant velocity between the surge and sway velocities). These relationships apply to all component connections in the entire train and ensure that the vehicle moves as one, both on straight and curved sections of track. It should be noted the wagon is modelled in this fashion also. The coupler spring stiffness is 1000 N/m and the damping coefficient is 50 Ns/m.

For the traction system, the locomotive has two DC motors that are dual shafted and each shaft is connected to the front and rear wheelsets through a gearing system with an overall reduction ratio G of 30:1, for four powered axles in total.

$$\omega_m = \omega_w G \tag{4}$$

$$\omega_w = \dot{s}_t/0.5d_w \tag{5}$$

Here, ω_m and ω_w are the rotational velocities of the motor and the wheelsets, respectively (rad/s) and d_w is the diameter of the wheels (0.055m). Due to the approximate conical shape of the wheels, the radius of the wheel would change depending on any hunting of the wheelset. This dynamic relationship is not modelled here. The current drawn by the motors can then be determined using the standard time-dependant current equation of a DC motor.

$$\frac{di}{dt}=\frac{V_c}{L}-\frac{Ri}{L}-\frac{K_e\omega_m}{L} \tag{6}$$

Here, i is the armature current (A), V_c is the voltage delivered by the controller (V), R is the armature resistance (1.5 Ω), K_e is the back-emf constant (0.01 V/rad/s) and L is the inductance (0.001 H). The surge (tractive) force is calculated using the motor torque and the wheel radius.

$$X_w = 2K_t i/0.5d_w \tag{7}$$

Here, X_w is the final surge force produced by each powered wheelset (N) and K_t is the torque constant (0.01 Nm/A). Note the doubling of this force since there are two wheels per wheelsets. Resistive forces are modelled as the standard train resistance equation based on empirical constants. These coefficients cover rolling resistance, flange contact and air resistance and are dependent on the speed of the train [6].

$$R = 1.1 + 0.14\dot{s}_t + 0.012\dot{s}_t^2 \tag{8}$$

$$R = 0.15 + 0.02\dot{s}_t + 0.004\dot{s}_t^2 \tag{9}$$

Here, Equation (8) is for the locomotive (N) and Equation (9) is for the wagon (N), respectively. This forms the resistance to motion of the entire vehicle.

2.3 Lateral Train Dynamics

Lateral dynamics for each component arise from the wheelset's interaction with curved track. The sway force for each component is trivial as it is taken to be the centripetal force that arises as each component enters and exits the curve. However, the yaw moment for each component varies based on which other components they are attached to. The wheelsets begin the chain reaction that eventually allows the entire vehicle to navigate the curve. The yaw moment for the wheelsets is governed by the time derivative of the curvature of the track and the velocity of the train [9].

$$N_W = J_W \dot{s}_t (\dot{\chi}) \tag{10}$$

Here, N_W is yaw moment acting on the wheelset (Nm), J_W is the yaw inertia of the wheelset (0.000018 kgm^2) and χ is the curvature of the track (1/m), which is the inverse of the curve radius R_{curve} (m). It should be noted that the wagon bogies also follow this relationship as the wheelsets are not modelled. In this case, the yaw inertia of the wheelsets is replaced with the yaw inertia for the wagon bogie frames (0.001 kgm^2). Equation (10) allows the wheelsets to gradually start aligning with the curve, which then begins to gradually align the bogie frames and carbody accordingly. To model the yaw moment for the bogie frames and the carbody, the relative yaw angle and yaw rate between two components (e.g. the leading wheelset and the leading bogie frame or the leading bogie frame of the wagon and the loaded container) are required.

$$\Delta\psi_1 = \psi_a - \psi_b \tag{11}$$

$$\Delta\dot{\psi}_1 = \dot{\psi}_a - \dot{\psi}_b \tag{12}$$

$$\Delta\psi_2 = \psi_a - \psi_c \tag{13}$$

$$\Delta\dot{\psi}_2 = \dot{\psi}_a - \dot{\psi}_c \tag{14}$$

Here, ψ and $\dot{\psi}$ are the yaw angle and yaw rate of the components in rad and rad/s, respectively. These are subscripted as a, b and c to indicate the interaction between multiple components e.g. the leading and trailing bogie frames and the carbody of the locomotive. The yaw moment can then be constructed based on these relationships.

$$N_{B,CB,WC} = (-k_\psi(\Delta\psi_1+\Delta\psi_2)-c_\psi(\Delta\dot{\psi}_1+\Delta\dot{\psi}_2))J_{B,CB,WC} \tag{15}$$

Here, $N_{B,CB,WC}$ is the yaw moment for either the locomotive bogie frames, the carbody or the container (Nm), k_ψ is the yaw stiffness (10 Nm/rad between locomotive wheelset and bogie frame, 100 Nm/rad between locomotive bogie and carbody and 50 Nm/rad between wagon bogie and container), c_ψ is the yaw damping (1 Nms/rad between locomotive wheelset and bogie frame, 10 Nms/rad between locomotive bogie and carbody and 5 Nms/rad between wagon bogie and container). The yaw inertia of the locomotive bogie frame is 0.001694 kgm^2, the locomotive carbody is 0.9 kgm^2 and the container is 0.04588 kgm^2, respectively.

2.4 Route Sub-Model

With the mathematical model in place, a test route with all the desired characteristics is required. The route used in this paper involves seven distinct parts. Firstly, a straight section of track of length 5m. This allows the train to reach cruising speed. Next, an ascending gradient of 1 in 60 (slope angle of approximately 0.95 degrees) of length 5m. This analyses the effects of each component's weight acting in opposition to the forces produced by the wheelsets. This is followed by a straight section of length 5m that will allow the train to exit the incline and settle at cruising speed again. Then a descending gradient of 1 in 60, again of length 5m. The gradients are followed by a straight section of length 5m to allow the train's speed to settle again. Next, a curved section of radius 0.92154m. This is in the shape of a quarter circle. This allows analysis of the effects of lateral dynamics on the vehicle and any decelerations resulting from curve negotiation (often termed curving resistance). Lastly, there is a final straight section of length 5m.

The route is deemed to be successfully navigated when the trailing bogie of the wagon exits the curve, where the simulation ends. It is taken that the speed restriction remains constant at 0.5 m/s over the entirety of the route, which allows the train to navigate the route in a reasonable time but also safely negotiate the curve without derailment occurring. It is important to distinguish between the speed restriction over the route and the desired speed for the train. Typically, a freight train driver operates at 90% of the overall speed restriction for the line [1]. This provides a buffer zone should the

driver need to increase speed. To determine a baseline for comparison, the route is simulated with no control structure, meaning the speed is not regulated.
The configuration of the train is one locomotive and one fully loaded Gondola wagon. The masses of each unit are 4.2kg (0.1 kg per wheelset, 0.4kg per bogie frame and 2.8kg for the carbody) and 1.85kg (0.025kg for each bogie frame and 1.8kg for the loaded container), respectively. A constant track voltage of 5.6V from the controller is set prior to the controller being moved from 'neutral' to 'forward.' This is the maximum voltage and therefore speed that the train can handle in the curve without derailing. This also sets the speed of the vehicle to be approximately 0.45 m/s, which equates to 90% of the quoted speed restriction. It is noted here that the minimum voltage required to move the train is 2V and the maximum voltage that the controller can deliver is 20V.

The mathematical model and route data is simulated in the MATLAB/Simulink environment. Due to the substantial number of components and therefore track parameters, MATLAB system objects are used so that changes made to any parameters are easily propagated to the relevant subsystems.

2.5 Inverse Simulation Framework

The control strategy of the train can be established using an IS framework. Conventional simulations involve the input of a tractive effort variable to a train performance model which produces the vehicle's dynamic response in terms of acceleration, speed and position [10]. Route parameters are then introduced when the vehicle encounters them. Quantities such as power and energy consumed for the journey can be calculated from these results. IS can be described as the reverse of this process, where the desired response of the vehicle forms the input to the inverse algorithm, producing an estimate of the required tractive effort from the traction system to traverse the route. For this application, tractive force is determined by the torque produced by the motors.

Several IS methods have been developed since its inception and have proven to be successful in several applications. These include the algorithms involving numerical differentiation and integration for discrete-time systems [11] and the feedback approach and approximate derivatives for continuous-time systems [12].

Only the feedback approach has been considered thus far for LTD. This has been successful in verifying the validity of the IS framework and for the study of Hydrogen Fuel Cell/Battery hybrid trains operating across routes in the Scottish Highlands [13]. The feedback approach for the train model is best explained for the linear time-invariant case using Laplace transform notation, but the method is not limited to linear models. The block diagram shown in Figure 2 contains the train model $G_t(s)$ and a feedback loop, where the error in the reference data and the model response is multiplied by a large gain factor $K_c(s)$.

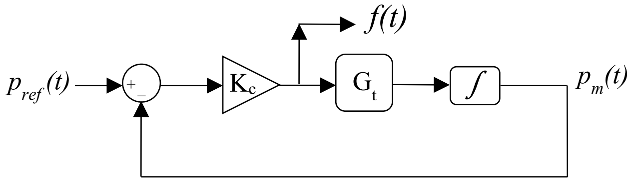

Figure 2: Feedback Principles IS Framework

The transfer function relating the predicted control input f(t) to a reference trajectory $p_{ref}(t)$ is given by:

$$\frac{F(s)}{P(s)} = \frac{1}{\frac{1}{K_c(s)} + G_t(s)} \tag{16}$$

A sufficiently large and tuned value for the gain ensures that the inverse of the gain tends to zero, which approximates the inverse model. Instability due to the use of feedback is not an issue for this application, although damped oscillatory transient responses are typical for the variables within the IS [10]. Since the goal of the IS based control system for the train is based on speed restriction adherence, the reference input is the desired speed profile. The input variable is the track voltage which is generated from the error between the reference speed and the train model speed.

$$V_c = K(\dot{s}_{ref} - \dot{s}_t) \tag{17}$$

Here, $\dot{s}_{ref}$ is the reference velocity for the train to follow (m/s) and K_c is the gain value (tuned to 500 for this application).

The simplest form of inputs involve a distance-time relationship or a constant value for the speed restriction. While this allows a quick setup of the IS, an issue arises in the opening phase of the simulation. Since the initial error in speed is equal to that of the speed restriction, the algorithm predicts maximum track voltage, which is not required. Therefore, a more gradual rise in the reference speed can be achieved by modelling the speed-time input as a standard decaying exponential function.

$$\dot{s}_{ref} = \dot{s}_{des}(1 - e^{-\sigma(t)}) \tag{18}$$

Here, $\dot{s}_{des}$ is the desired train speed, which is derived in Section 2.4 (m/s), σ is the factor which determines the time constant for the profile and t is the simulation time (s). It should be noted here that integrating the response from Equation (18) produces the corresponding distance-time profile. However, as observed in previous work, there appears to be no discernible difference in a distance or speed profile [10]. However, the use of a distance-time profile is perhaps more desirable as train schedules are normally provided this way. A value of 8 for σ is chosen as it allows the train to reach cruising speed quickly without causing issues in the track voltage prediction. The variation of input trends for the IS highlights another advantage. The acceleration of the vehicle can be directly controlled by altering the severity of the gradient of the speed-time input by modifying Equation (18). This is useful for ensuring the locomotive does not induce harmful forces on the couplers by attempting to accelerate too quickly when pulling many wagons. Also, the speed increases and decreases can be altered to allow for poor adhesion conditions so that significant wheel slip is avoided. Different performance curves in terms of speed can be seen below in Figure 3.

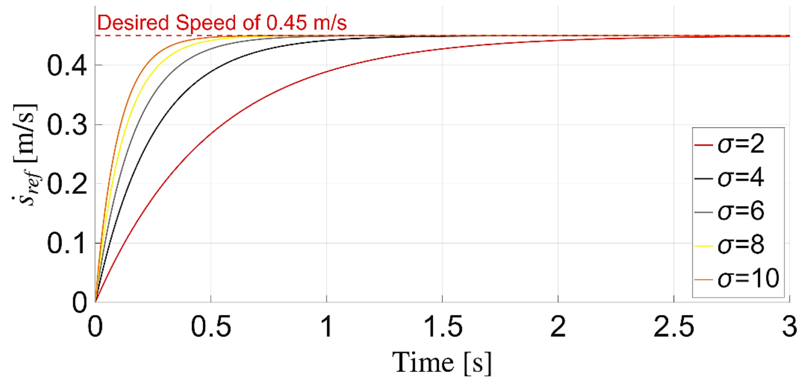

Figure 3: Different Performance Curves

3 Results

The responses provided here are the responses of the carbody of the locomotive. The speed response for the forward simulation is given below in Figure *4*.

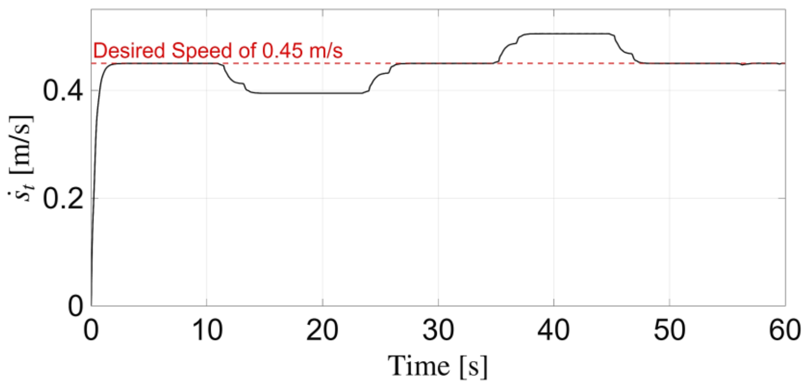

Figure 4: Speed Time History for the Forward Simulation

The speed settles at a value of 0.45 m/s after the initial acceleration phase. Speed then begins to drop in a stair-like fashion as the train enters the incline. Each drop in speed corresponds to a successive component entering the incline and the gradient force taking effect. The train settles at a speed of 0.39 m/s when on the incline and accelerates to 0.45 m/s again after reaching the top of the incline. The speed then rises in a stair-like fashion again as the train navigates the descending gradient. The train settles at a speed of 0.51 m/s, which exceeds the speed restriction. The train takes longer to navigate the ascending gradient than the descending gradient due to the train's weight acting as a resistive component of force on the ascending gradient and a propulsive force on the descending gradient. Finally, the curve causes some minor transient decelerations, with a maximum speed drop to 0.447 m/s observed upon entry to the curve. The tractive effort generated from the wheelsets mimics this behaviour and is shown below in Figure 5.

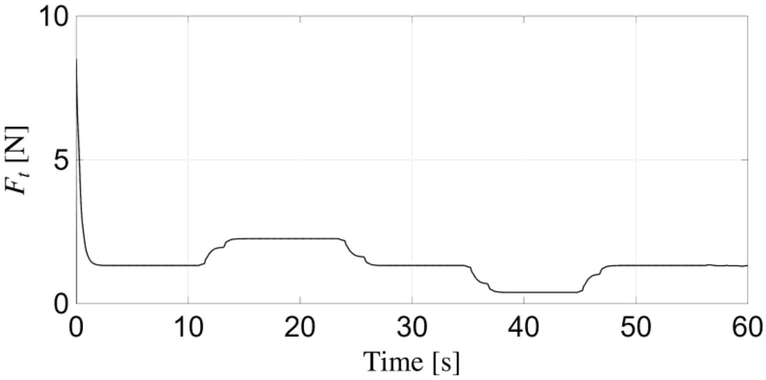

Figure 5: Tractive Force from the Forward Simulation

The tractive force settles at a constant value after the initial spike as the forces of friction and air resistance are balanced with the traction force. The tractive force then rises and falls in accordance with the gradient and curve in a similar fashion to the speed. The inertial positions are provided below in Figure 6.

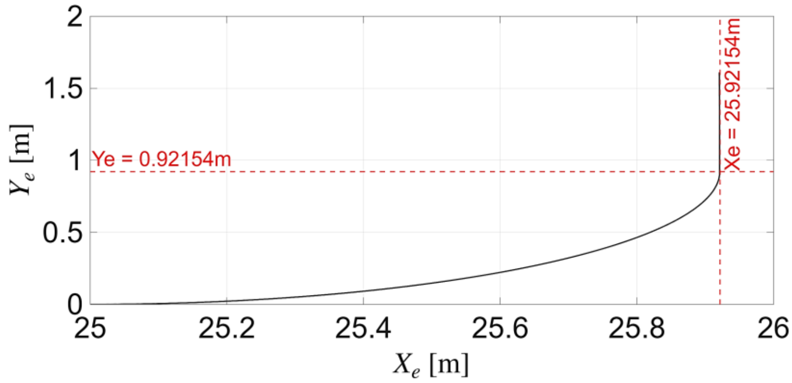

Figure 6: Positions for the Forward Simulation

The position time histories confirm that the train has completed the route. When the train enters the curve, the longitudinal position decreases and settles at 25.92154m, while the lateral position begins to increase. This is expected as the radius of the curve is 0.92154m. The quarter circle curve is navigated correctly as both the longitudinal and lateral positions are as expected. The same set of results are now provided for the IS. The speed response is given below in Figure *7*.

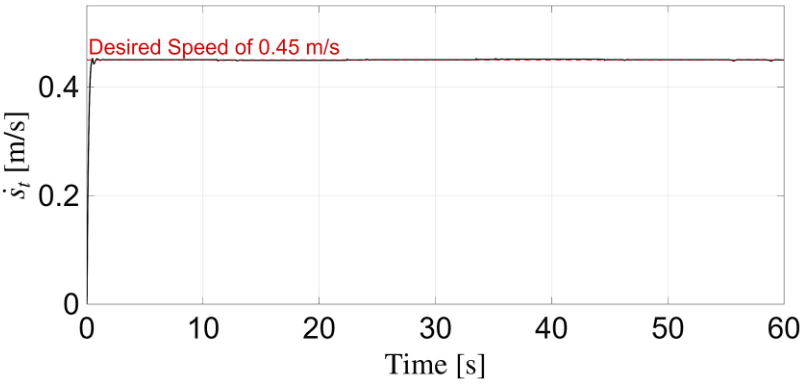

Figure 7: Speed Time History for the IS

It is clear from the speed profile obtained from the IS that the speed restriction is adhered to much more effectively than that of the forward simulation. Some minor increases are observed at the instances where the train is entering/exiting the various parts of the route, but these are quickly dealt with. This was not the case in the forward simulation, where the speed of the vehicle was constantly under threat from the track features. The tractive force and track voltage time histories are given below in Figure *8* and Figure *9*, respectively.

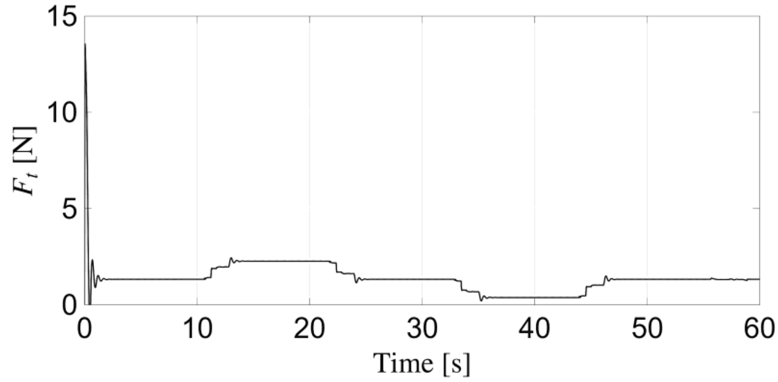

Figure 8: Tractive Force for the IS

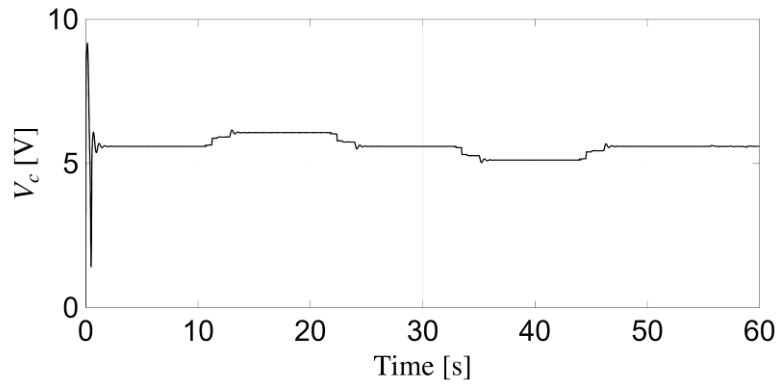

Figure 9: Track Voltage Prediction for the IS

The tractive force emulates that of the forward simulation, but there are marginal differences that ensure the train adheres to the speed restriction. For example, for the incline, the tractive force settles at 2.27N for the IS, in contrast to 2.26N for the forward simulation. The track voltage begins with some oscillatory transient behaviour before settling at a value of 5.6V, which is equivalent to the forward simulation However, the main advantage of the IS can be seen once the train enters the incline, where the voltage is increased in a stair like fashion like the speed drops observed in the forward simulation. The voltage required to maintain a speed of 0.45 m/s on the ascending gradient is predicted to be 6.07V and the voltage required to maintain speed on the descending gradient is 5.12V. A small increase in voltage is observed when the train enters the curve, but this is negligible in comparison to the voltage changes required for the gradients. Finally, there are several instances of oscillatory transients observed throughout the voltage prediction. Due to the nature of the multi-dynamic digital twin used in this paper, the track voltage rises in accordance with successive components entering the incline. Smaller rises are needed for the wheelsets and bogie frames, and larger jumps are needed for the carbody and fully loaded wagon container. The position time histories are given below in Figure 10.

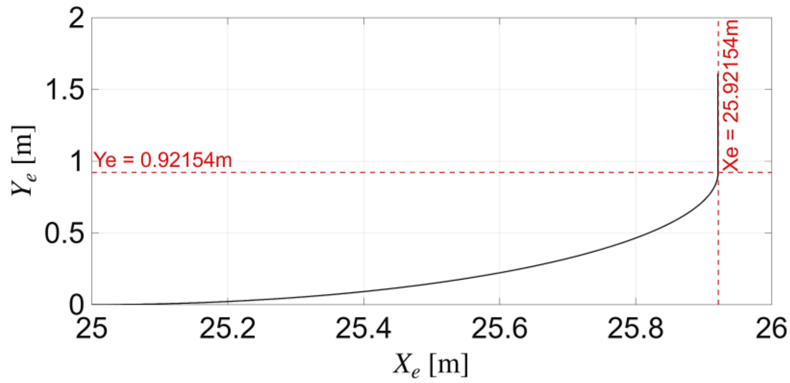

Figure 10: Positions for IS

The position trends are provided to verify that the route has been successfully completed. Once again, the quarter circle curve has been traversed successfully. It is worth noting that the journey times from the forward and inverse approaches are similar but not identical. Primarily this difference is because there is no speed regulation in the forward simulation, which allows the train to exceed the speed limit when travelling downhill, contributing to the slightly reduced journey time in comparison to the inverse model. However, the overall difference of approximately 2s is negligible in terms of scheduling purposes. This is a bonus of the IS framework.

4 Conclusions and Contributions

The primary contributions are:

- The first iteration of a LTD model that evolves the standard combined and distributed mass models. This offers additional insight into how the vehicle traverses various track topologies and how the resistive forces gradually apply to the vehicle.

- The development of a IS framework that can be applied to any track profile and train configuration. Speed control was achieved over the route, where there were minimal deviations from the desired speed, even in the presence of challenging gradients and curves.
- The use of a G-Scale model railway in the context of rail vehicle dynamics and control to try and reduce the uncertainties that can arise from the estimation of traction behaviour for a full-scale freight train.

Acknowledgements

The authors would like to thank the Chancellor's Fund at the University of Glasgow for providing some funds to purchase the model railway equipment.

References

[1] M. Saadat, M. Esfahanian, M. Saket, "Reducing fuel consumption of diesel-electric locomotives using hybrid powertrain and fuzzy look-ahead control", Proceedings of the Institution of Mechanical Engineers, Part F: Journal of Rail and Rapid Transit, 231(4):406-418, 2016, DOI:10.1177/0954409716631010.

[2] Q.Wu, M. Spiryagin, C. Cole, "Longitudinal train dynamics: an overview", Vehicle System Dynamics, *54*(12), 1688-1714, 2016, DOI:10.1080/00423114.2016.1228988

[3] D. J. Murray-Smith, "Feedback methods for inverse simulation of dynamic systems for engineering applications, Mathematical and Computer Modelling of Dynamical Systems", 175(5), 515-541, 2011, DOI:10.1080/13873954.2011.584323

[4] Anonymous, "Highland Rail Room for Growth Study", Highlands and Islands Enterprise, Accessed 24 May 2024.

[5] M. Chou, X. Xia, C. Kayser, "Modelling and model validation of heavy-haul trains equipped with electronically controlled pneumatic brake systems", Control Engineering Practice, 15(4), 501-509, 2007,DOI: 10.1016/j.conengprac.2006.09.006.

[6] T.I. Fossen, "Guidance and Control of Ocean Vehicles", Wiley and Sons Ltd, 1994. DOI: 10.1016/0005-1098(96)82331-4.

[7] E.W. McGookin, "Optimisation of Sliding Mode Controllers for Marine Applications: a Study of Methods and Implementation Issues", Glasgow, University of Glasgow, 1997.

[8] S. R. K. Shilliday, E. W. McGookin and D. G. Thomson, "A Comparison of Forward and Inverse Simulation Methods for Fault Detection on a Rover," 8th International Conference on Control, Decision and Information Technologies *(CoDIT)*, 1432-1437, 2022,DOI:10.1109/CoDIT55151.2022.9804106

[9] V. K. Garg, R. V. Dukkipati, "Chapter 8 - Response of Railway Vehicles on Curved Track, Dynamics of Railway Vehicle Systems", Academic Press, 263-331, 1984, DOI:10.1016/B978-0-12-275950-5.50013-4.

[10] D.J. Murray-Smith, "Development of an inverse simulation method for the analysis of train performance", Proceedings of the Institution of Mechanical Engineers, Part F: Journal of Rail and Rapid Transit, 232(5), 1295-1308, 2017, DOI:10.1177/0954409717720349.

[11] D.Thomson, R.Bradley, "Inverse simulation as a tool for flight dynamics research – principles and applications", Progress in Aerospace Sciences, 42(3), 174-210, 2006, DOI:10.1016/j.paerosci.2006.07.002.

[12] D.J. Murray-Smith, E.W. McGookin, "A case study involving continuous system methods of inverse simulation for an unmanned aerial vehicle application", Proceedings of the Institution of Mechanical Engineers, Part G: Journal of Aerospace Engineering, 229(14), 2700-2717, 2017, DOI:10.1177/0954410015586842.

[13] D.J. Murray-Smith, "Design options for hybrid trains powered by hydrogen fuel cells and batteries for routes in the Highlands of Scotland. Results for the case of a three-coach multiple-unit train", Technical Report, Scottish Association for Public Transport, Glasgow.